



**NUMERICAL INVESTIGATION ON BEHAVIOUR OF COLD-FORMED STEEL
BUILT-UP COLUMN WITH WEB PERFORATIONS**

Dyanesh T ¹

1 PG Structural Engineering Student, Government College of Technology, Coimbatore,
Tamil Nadu, India.
dyanesh221098@gmail.com

Rama M ²

2 Associate Professor, Government College of Technology, Coimbatore, Tamil Nadu, India.
mrama@gct.ac.in

Karthik C ³

3 Associate Professor, Velalar College of Engineering and Technology, Erode, Tamil Nadu, India.
ckarthik.strl@gmail.com

Received: 30/08/2024

Revised: 22/12/2024

Accepted: 01/02/2025

ABSTRACT

Cold-Formed Steel (CFS) channel sections are increasingly being employed in structures to handle weights-to-strength ratio. The web perforations are often punched to limiting their size and reduce the section weight to some extent. Back-to-back CFS lipped channels with edge-stiffened holes are an innovative kind of structural element, to be more efficient than regular CFS channels with unstiffened holes. This study delivers the findings of 15 parametric results on the axial strength of back-to-back lipped channels with edge-stiffened holes, un-stiffened holes and plain webs. Nonlinear elastoplastic finite element model was analyzed and it agreed well with the test results. When compared to a back-to-back lipped plain channel section, a built-up lipped channel section with seven edge-stiffened web apertures displayed a better improvement in compression resistance and the same section with the same number of unstiffened web openings experienced a significant reduction in compression resistance. The design strength of the sections was calculated through BS5950-5:1998 and assessed. By incorporating seven edge-stiffened web perforations, there was 10% decrease in the overall size of the member, enabling weight reduction without compromising major structural integrity. Web perforated sections are reduced the structural weight; it may reduce the shear resistance caused by wind and seismic effect.

Keywords: Cold-formed steel, Lipped channel section, Perforated section, Edge-stiffened holes, Finite element analysis.

I. INTRODUCTION

In the field of structural engineering, the choice of materials plays a pivotal role based on strength, ductility, maintenance and durability aspects. One category of materials that has gained significant attention is Cold-Formed Steel (CFS). CFS distinct from its hot-rolled counterpart, is manufactured through a unique process that imparts distinctive properties to the material. The web perforation concept has several advantages over traditional built-up channel sections due to its aesthetic appeal, light and shadow play, Ventilation and Acoustics, Reduced material usage, Design flexibility are some of the

advantages of perforated structural steel columns which finds application across a spectrum of industries, residential and commercial construction, good corrosion resistance, simplicity of maintenance and excellent fire resistance which were observed Dang et al. and Dar et al. (2021).

The research landscape surrounding the behaviour of Cold-Formed Steel Columns (CFSC) under axial load has witnessed significant exploration, as highlighted in recent literature. Shabhari et. al. (2024) conducted an experimental and numerical investigation with lipped channel stub columns to understand the influence of perforation in the local buckling behaviour and proposed a design curve by considering perforation effect. Zhang et. al. (2024) performed tests, numerical analysis on web-stiffened C-section columns and identified that web stiffened sections are exhibited intensified deformation post-perforation, reducing their axial stiffness and load-bearing capacity and proposed strength reduction factor. Elham et al. (2024) performed parametric study about the impact due to lateral load on axially loaded cold-formed concrete filled columns and suggested that the wall thickness of the column plays a vital role in the column load carrying capacity. Karthik et. al. (2024) proposed a design rules based on their experimental and parametric study for cold-formed ferritic stainless steel closed built-up beams. Warda et al. (2024) were preferred ABAQUS for Finite Element Analysis (FEA) due to its depth in robust nonlinear analysis capabilities, advanced material modelling and it is ease in user support for complex simulations. Zhao et. al. (2023) Cold-formed steel channel sections with and without slotted web holes were tested under pinned-pinned boundary conditions and discussed about the element failures. Wang et. al. (2022) compression behaviour of perforated cold-formed beams-columns with longitudinal web stiffeners, complex edge stiffeners were experimentally studied and concluded that the DSM result was closer to the experimental result. Dang et al. (2021) conducted a review encompassing compression tests and FEA using ABAQUS to investigate the buckling behaviour of CFSC, particularly focusing on columns with perforations. The findings underscored the influence of slenderness, thickness, temperature and the presence of holes on buckling modes, with perforated RHS columns frequently succumbing to local buckling. Guo et al. (2021) and Yao (2021) examined the design approach for CFS lipped channel stud columns with web holes, suggesting criteria based on hole

dimensions to enhance structural performance. Ebrahim et al. (2020) numerically investigated and concluded that the shape, size of the openings has also a significant effect on the seismic behaviour and the ultimate capacity of the perforated structures. Chen et al. (2019, 2020a & 2020b) conducted parametric studies with lipped channel section considering the factors like beam length and hole diameter on compression capacity. Chungang et al. (2019) experimentally and numerically Investigated Perforated CFS Built-up I-Section Columns with web stiffeners and complex edge stiffeners led to predicting the web crippling strength. Roy et al. (2019) investigated by both experiments and numerical of screw pattern of self-drilling screw connections for high strength cold-formed steel. Athira et al. (2018) studied the impact of perforation shapes in C and Z sections, emphasizing stress concentration effects on buckling loads. Kulatunga and Macdonald (2013, 2014 & 2019) examined the load carrying capacity of lipped channel members with perforations, with results indicating significant variations based on perforation placement. Yao et al. (2017) carried parametric study on Perforated CFS Members in compression. Xu et al. (2014) observed the compressive strength of CFS C-shape columns with slotted holes. Cristopher D. Moen and B.W. Schafer (2008) investigated the elastic buckling behaviour of CFSC with holes, establishing correlations between local, distortional, and global buckling responses.

Research gaps exist to understand the effects of edge-stiffened openings on compression members and limited exploration of built-up channel sections with perforations. In this study, Plain, web perforated with and without edge stiffened column sections with various lengths were analysed to understand the behaviour. Finite element tool ABAQUS was used to perform the non-linear analysis. The impact of the web perforations on load-bearing capacity, buckling characteristics and failure modes of CFS columns are studied.

II. METHODOLOGY

From the literature study, found that the limited data were available for edge-stiffened built-up channel sections with perforations under axial loading condition. In this study, the FEA are performed with FE tool ABAQUS to get more precious results. The geometric dimensions of the perforated edge-stiffened built-up channel sections and material properties were obtained from literature to validate FEA

results. Further, parametric studies have been carried out to explore the impact of varying parameters such as length of the specimen, perforation at web and stiffeners at hole location. The results are discussed to draw engineering conclusions.

III. NUMERICAL STUDY

A. Geometric Limitations:

The section dimensions were selected based on grade specified in as per Australian/New Zealand Standard, Cold Formed Steel structures - AS/NZS 4600:2005. The concept of web perforated built-up channel section carried in this studied is shown in **Error! Reference source not found.**

B. Section Labelling:

Labels clearly identify the sample itself, including geometric or chemical property details Both validated and parametric specimens were labelled. For example, the specimens were labelled as C190×45×15-t1.5-L1500-NH0-01, from which the first three terms indicated the cross-sectional dimensions of web depth, flange width and height of lip. The terms t1.5 indicates the thickness of the section, L1500 is the effective length, NH0 means that no hole at the web. The last term indicates that the repeatability of the section. Similarly, EH1 is the edges are stiffened and UH1 is the edges are unstiffened.

C. FEA Model:

For simulation of complex geometries with different material properties under various loading conditions, numerical solutions were obtained with the help of Finite Strip Method (FSM) and Finite Element Method (FEM). In this study, CUFSM is free and open-source software that is used to investigate the elastic buckling of any CFS cross-section using the finite strip and ABAQUS standard version is employed as a finite element tool.

D. Geometrical imperfections:

The initial local geometrical imperfections are developed in the section walls at the time of plate production and fabrication, it significantly involve the behaviour and strength of the section. In this study, the local geometric imperfections were incorporated in the FE model. The lowest buckling mode

shape was imported from the linear analysis and it is used for non-linear analysis. In the parametric models, the local geometrical imperfection value of $0.34t$ was used.

E. Validation:

The FE modelling approach has been validated with experimental results of axial strength of back-to-back CFS channels with edge-stiffened holes, un-stiffened holes and plain webs reported by Chen et al. (2020). The cross section and the web hole locations of validated built-up channel column are shown in **Error! Reference source not found.** The material properties considered are tabulated in

Table I. The comparison between the ultimate load of the tested specimens and those computed by the FEA are shown in *Table II*. It shows a reasonable agreement between the numerical and test results. The mean and standard deviation for P_{U-TEST}/P_{U-FEA} is 0.996 and 0.020. The buckling modes between the tested specimens and obtained from FEA are shown in **Error! Reference source not found.** The numerical results show a reasonable agreement with test results.

F. Parametric Study:

A total of 15 FE models of built-up channel section with Plain, Unstiffened and Edge stiffened holes of lengths of 750 mm, 1300 mm and 1500 mm, thickness 1.6 mm, having cross-sections with (d/b_f) ratio 0.47 were analyzed in the ABAQUS. The material properties for CFS sections are obtained from the Effects of edge-stiffened web openings on the behaviour of CFS channel sections under compression reported by Chen et al. (2020). The material properties for the built-up channel column for parametric study were shown in *Table III*. The FE model includes the material non-linearity, geometric non-linearity and geometric imperfections. All the sections are complied with Australian/New Zealand Standard and specification and are within the recommended limitation value. The cross section and the web hole location of built-up channel column for parametric study are shown in **Error! Reference source not found.** The web perforation locations are shown in **Error! Reference source not found.** The ultimate load of the parametric sections is shown in

Table IV.

G. Effective Width Method as per BS5950-5:

The load carrying capacity (P_{U-BS}) of column was calculated based on clause 6.2.2 of BS5950-5:1998. The local buckling stress, flexural, torsional, torsional flexural buckling capacity of the column was calculated based on the equations 1 to 4. The parametric columns are mainly failed by combination of torsional flexural buckling.

$$N_{cr,f} = 0.904EK \left(\frac{t}{b} \right)^2 \quad 1$$

$$N_{cr,F} = \frac{\pi^2 EI_x}{L_E^2} \quad 2$$

$$N_{cr,T} = \frac{1}{i_0^2} \left(GJ + \frac{\pi^2 EC_w}{L_E^2} \right) \quad 3$$

$$N_{cr,TF} = \frac{1}{2\beta} \left[(N_{cr,F} + N_{cr,T}) - \sqrt{(N_{cr,F} + N_{cr,T})^2 - 4\beta N_{cr,F} N_{cr,T}} \right] \quad 4$$

H. Results and Discussions:

The FEA results of parametric sections are shown in

Table IV. It is observed that the curves at elastic range and ultimate load are almost same to that of the validation model with minor variation. But the slight deviation of curves in the graph may be due to imperfections considered. From the result, it is observed that the back-to-back channel sections with 1 edge stiffened holes and 7 edge stiffened hole gains 32.5% and 45.9% than the same plain section. Also, the channel section with 1 unstiffened hole and 7 unstiffened holes retards 18.7% and 24.5% respectively than the same plain section. It has been also observed that 1500 mm length section with seven perforation shows higher strength than the single perforation which is due to reduced stress concentration, improved load distribution and reduced web buckling which is caused by stiffening ribs across the section.

From the

Table IV, It was observed that the Effective Width Method (EWM) as per BS5950-5 performs effectively in predicting buckling behaviour with the mean and standard deviation of 1.02 and 0.172 respectively. All the parametric sections are failed by combination of torsional flexural buckling. But, lack of design procedure is available to calculate the distortional buckling capacity by EWM.

The **Error! Reference source not found.** represents axial shortening verses axial Load for critical built-up channel section BC190×45×15-t1.6-L1500-NH0, BC190×45×15-t1.6-L1500-UH1, BC190×45×15-t1.6-L1500-EH1 and BC190×45×15-t1.6-L1500-EH7. From the Figure 6, it was observed that the axial shortening and the corresponding load values for each section which shows that shortening rate increases with increase in the loading till ultimate capacity. Later on, both are mutually decreases with same mode as before to failure load. The strength increment for seven web perforations is significantly higher than the strength increment for single perforation which is because the multiple web perforations provide additional web stiffness, reduce the effective slenderness ratio of the web, and increase the shear strength of the web. As the buckling mode for 750 mm, 1300 mm & 1500 mm length sections are reported to be as local, distortional and global respectively, it is observed to be the same as followed in this study also. The corresponding buckling modes for the sections BC190×45×15-t1.6-L1500-NH0, BC190×45×15-t1.6-L1500-UH1, BC190×45×15-t1.6-L1500-EH1 and BC190×45×15-t1.6-L1500-EH7 are shown in below **Error! Reference source not found.**. The section having length 1500 mm shows global buckling, it tends to buckle at its mid portion irrespective of perforations, which was also clearly depicted in below **Error! Reference source not found.**.

One perforation at web with edge stiffened section produced higher axial load carrying capacity than plain sections and un-stiffened sections. It clearly states that the edge stiffened is effective to carry higher load carrying capacity. The multiple holes on web significantly produce the lessor axial load, however holes with edge stiffened sections produce higher axial load carrying capacity.

IV. CONCLUSION

This study includes a comprehensive investigation comprising numerical and experimental methodologies to analysis the buckling behaviour of CFS built-up column with web perforations. While

the numerical study provides computational insights, the and experimental data is aim to validate. Fifteen back-to-back channel sections with plain, unstiffened and edge stiffened web holes to drawn the conclusion. The behaviour of the built-up columns is significantly influenced by the size and form of the web perforations, the length and thickness of the edge stiffeners, the placement of the perforations in the web, cross-sectional design, member length, and the loading circumstances. In Cold Formed Steel built-up columns with web perforations, edge stiffeners with higher perforation number (7 nos.) can greatly increase the web crippling strength by 45.9% and unstiffened perforation (7 nos.) with decreased web crippling strength by 24.5% than the plain sections of same dimension. As length increases strength decreases which has been recovered by using the edge stiffened perforation condition. The strength increment for seven web perforations over a single perforation is due to a combination of factors, including web stiffening, reduced centroid shift, improved load distribution, and increased effective area. Seven numbers of edge stiffened web perforation, it was about 10% reduction in overall member size which can help to reduce the weight of a section by removing material does not affect the major structural integrity of the section. Also reduces cost in fabrication, transportation, operation and maintenance. This perforation on the elements reduced the structural weight; it may reduce the shear resistance caused by wind and seismic effect.

This study collectively contributes to understanding the complex behaviour of CFS built-up sections with perforations, providing insights into design considerations as per BS5950-5, structural performance, and failure mechanisms. Edge-stiffened openings enhance compression resistance. However, increased column slenderness decreases axial capacity. Overall, the findings of this investigation suggest that edge-stiffened web openings may increase the compression resistance of CFS lipped built-up channel sections significantly. However, more research is needed to develop accurate design equations for these lipped built-up channel sections.

NOMENCLATURE

A	=	Cross-sectional area;
a	=	Diameter of the perforation;
b_f	=	Breadth of flange;
b_L	=	Overall depth of lip;
C_w	=	Warping constant;
d	=	Overall depth of the section;
E	=	Young's modulus of elasticity;
f_y	=	Yield stress;
G	=	Shear modulus;
I	=	Second moment of the area;
I_o	=	Polar radius of gyration about the shear centre;
J	=	St Venant torsion constant;
K	=	Local buckling coefficient;
L (or) L_E	=	Effective length of member;
$N_{cr,f}$	=	Local buckling stress;
$N_{cr,F}$	=	Elastic flexural buckling load of a column;
$N_{cr,T}$	=	Torsional buckling load of a column;
$N_{cr,TF}$	=	Torsional flexural buckling load of a column;
P_{U-TEST}	=	Ultimate strength obtained from experimental work;
P_{U-FEA}	=	Ultimate strength obtained from Finite Element analysis software ABAQUS;
P_{U-BS}	=	Design strength calculated as per BS5950-5:1998;
q	=	Width of edge stiffener;
R	=	Corner radius of the section;
t	=	Thickness of the section;
$\sigma_{0.2}$	=	0.2% proof stress;
σ_u	=	Ultimate tensile strength of material;
β	=	Torsional constant;

REFERENCES

- [1] Athira V.V., & Sruthy S. (2018). "Investigation on the use of cold formed perforated steel sections as columns and purlins", *International Journal of Engineering & Technology*, 7(4.5), 716. <https://doi.org/10.14419/ijet.v7i4.5.25066>.
- [2] Amoke Shabhari., Vijaya Vengadesh Kumar Jeyapragasam., & Chandrasekar, D. (2024). "Local buckling behaviour of web perforated cold-formed steel lipped channel columns", *Thin-Walled Structures*, 205(B), 112448. <https://doi.org/10.1016/j.tws.2024.112448>.
- [3] Chungang Wang., Shanshan Li., Zhuangnan Zhang., Haokai Qian., & Yuting Guo. (2022). "Experiments on perforated cold-formed built-up I-section beam-columns with longitudinal web and complex edge stiffeners", *Structures*, 38, 765-780. <https://doi.org/10.1016/j.istruc.2022.02.011>.
- [4] Chen, B., Roy, K., Uzzaman, A., Raftery, G., & Lim, J. B. P. (2020a). "Axial strength of back-to-back cold-formed steel channels with edge-stiffened holes, un-stiffened holes and plain webs", *Journal of Constructional Steel Research*, 174, 106313. <https://doi.org/10.1016/j.jcsr.2020.106313>.
- [5] Chen, B., Roy, K., Uzzaman, A., Raftery, G. M., & Lim, J. B. P. (2020b). "Parametric study and simplified design equations for cold-formed steel channels with edge-stiffened holes under axial compression", *Journal of Constructional Steel Research*, 172, 106161. <https://doi.org/10.1016/j.jcsr.2020.106161>.
- [6] Chen, B., Roy, K., Uzzaman, A., Raftery, G. M., Nash, D., Clifton, G. C., Pouladi, P., & Lim, J. B. P. (2019). "Effects of edge-stiffened web openings on the behaviour of cold-formed steel channel sections under compression", *Thin-Walled Structures*, 144, 106307. <https://doi.org/10.1016/j.tws.2019.106307>.
- [7] Dang, E. R., & Jamaluddin, N. (2021). "A Review on the Experimental Study of Cold-Formed Steel Columns with Holes subjected to an Axial Load", *Recent Trends in Civil Engineering and Built Environment*, 2(1), 330–339. <https://doi.org/10.30880/rtcebe.2021.02.01.036>.
- [8] Dar, A. R., Karthik, C., Anbarasu, M., & Dar, M. A. (2021). "Testing of cold-formed ferritic stainless steel stub columns: axial behaviour and design strengths", *Innovative Infrastructure Solutions*, 6(3), 176. <https://doi.org/10.1007/s41062-021-00541-w>.
- [9] Ebrahim Zamani Bevdokhti., & Hashem Khatibi. (2020). "Improving Cyclic Behaviour of Steel Plate Shear Walls with Elliptical Perforations", *Civil Engineering Infrastructures Journal*, 53(1), 89–102. <https://doi.org/10.22059/cej.2019.276064.1553>.
- [10] Elham Ghandi., Nayyer Mohammadi Rana., & Shirin Esmaeili Niari. (2024). "Parametric Analysis of Axially Loaded Partially Concrete-Filled Cold-Formed Elliptical Columns Subjected to Lateral Impact Load", *Civil Engineering Infrastructures Journal*, Article in press, Available online from 04th February. <https://doi.org/10.22059/cej.2024.364758.1955>.
- [11] Gardner, L., & Yun, X. (2018). "Description of stress-strain curves for cold-formed steels", *Construction and Building Materials*, 189, 527–538. <https://doi.org/10.1016/j.conbuildmat.2018.08.195>.
- [12] Guo, Y., & Yao, X. (2021). "Experimental Study and Effective Width Method for Cold-Formed Steel Lipped Channel Stud Columns with Holes", *Advances in Civil Engineering*, 2021, 1–16. <https://doi.org/10.1155/2021/9949199>.
- [13] Hoseinpoor, A., & Tafti, J. (2017). "Cyclic Loading Tests for Cold-Formed Steel Wall Frames with Lightweight Concrete", *Civil Engineering Infrastructures Journal*, 50(1), 119–133. <https://doi.org/10.7508/cej.2017.01.007>.

- [14] Jia-Hui Zhang., Jiaxin Wang., Shuluan Xu., & Fangying Wang. (2024). “Testing, numerical modeling and design of perforated advanced high-strength steel channel section columns”, *Journal of Constructional Steel Research*, 214, 108440. <https://doi.org/10.1016/j.jcsr.2023.108440>.
- [15] Jinyou Zhao., Shuo Liu., & Boshan Chen. (2023). “Axial strength of slotted perforated cold-formed steel channels under pinned-pinned boundary conditions”, *Journal of Constructional Steel Research*, 200, 107673. <https://doi.org/10.1016/j.jcsr.2022.107673>.
- [16] Karthik, C., Anbarasu, M., & Mohammad Adil Dar. (2024). “Reliable design rules for cold-formed ferritic stainless steel closed built-up beams”, *Advances in Structural Engineering*, 27(5), 722-742. <https://doi.org/10.1177/13694332241232046>.
- [17] Kulatunga, M. P., & Macdonald, M. (2013). “Investigation of cold-formed steel structural members with perforations of different arrangements subjected to compression loading”, *Thin-Walled Structures*, 67, 78–87. <https://doi.org/10.1016/j.tws.2013.02.014>.
- [18] Kulatunga, M. P., Macdonald, M., Rhodes, J., & Harrison, D. K. (2014). “Load capacity of cold-formed column members of lipped channel cross-section with perforations subjected to compression loading – Part I: FE simulation and test results”, *Thin-Walled Structures*, 80, 1–12. <https://doi.org/10.1016/j.tws.2014.02.017>.
- [19] Macdonald, M., Kulatunga, M. P., & Kotelko, M. (2019). “The effects of compression loading on perforated cold-formed thin-walled steel structural members of lipped-channel cross-section”, *AIP conference proceedings*, 020007, 1-10. <https://doi.org/10.1063/1.5086138>.
- [20] Moen, C. D., & Schafer, B. W. (2008). “Experiments on cold-formed steel columns with holes”, *Thin-Walled Structures*, 46(10), 1164–1182. <https://doi.org/10.1016/j.tws.2008.01.021>.
- [21] Roy, K., Lau, H. H., Huon Ting, T. C., Masood, R., Kumar, A., & Lim, J. B. P. (2019). “Experiments and finite element modelling of screw pattern of self-drilling screw connections for high strength cold-formed steel”, *Thin-Walled Structures*, 145, 106393. <https://doi.org/10.1016/j.tws.2019.106393>.
- [22] Warda Badis., Menadi Belkacem., & Rafik Taleb. (2024). “Numerical Simulation of Local Reinforcement of Steel Column-Beam Connections”, *Civil Engineering Infrastructures Journal*, Article in press, Available online from 08th October. <https://doi.org/10.22059/cej.2024.377321.2077>
- [23] Wang, C., Guo, Q., Zhang, Z., & Guo, Y. (2019). “Experimental and numerical investigation of perforated cold-formed steel built-up I-section columns with web stiffeners and complex edge stiffeners”, *Advances in Structural Engineering*, 22(10), 2205–2221. <https://doi.org/10.1177/1369433219836174>.
- [24] Xu, L., Shi, Y., & Yang, S. (2014). “Compressive Strength of Cold-Formed Steel C-shape Columns Compressive Strength of Cold-Formed Steel C-shape Columns with Slotted Holes with Slotted Holes”, *Scholars Mine*. <https://scholarsmine.mst.edu/isccss/22iccfss/session02/4>.
- [25] Yao, X. (2021). “Experimental Study and Proposal to Improve the EWM Design of Cold-Formed Steel Lipped Channel Columns with Circular Holes under Axial Compression”, *Advances in Materials Science and Engineering*, 1–21. <https://doi.org/10.1155/2021/9389121>.
- [26] Yao, Z., & Rasmussen, K. J. R. (2017). “Perforated Cold-Formed Steel Members in Compression. I: Parametric Studies”, *Journal of Structural Engineering*, 143(5). [https://doi.org/10.1061/\(ASCE\)ST.1943-541X.0001635](https://doi.org/10.1061/(ASCE)ST.1943-541X.0001635).
- [27] BS 5950-5:1998 - Code of practice for design of cold formed thin gauge sections, British Standard Institution, United Kingdom.

- [28] BS EN, Tensile Testing of Metallic Materials Method of Test at Ambient Temperature, British Standards Institution, 2001.
- [29] IS: 801 – 1975 (Reaffirmed 2010) - Indian Standard code of practice for use of cold-formed light gauge steel structural members in general building construction (First Revision), India.
- [30] ABAQUS Analysis User's Manual-Version 6.14-2, ABAQUS Inc., United States of America, 2018.

NUMERICAL INVESTIGATION ON BEHAVIOUR OF COLD-FORMED STEEL BUILT-UP COLUMN WITH WEB PERFORATIONS

Table I. Material properties for validated specimens

Coupon ID	Coupon location	$\sigma_{0.2}$ N/mm ²	σ_u N/mm ²
B240-t1.75-F	Flat	317.33	402.57
B240-t1.75-C	Corner	348.9	412.5

Table II. Comparison of ultimate load capacity between test and FEA for the validated specimens

Specimen ID (as per Literature)	P_{U-TEST} (kN)	P_{U-FEA} (kN)	P_{U-TEST}/ P_{U-FEA}	Remarks
B240×t1.75-L420-S100-NH0	194.8	199.4	0.98	Plain Section
B240×t1.75-L920-S100-NH0	171.8	178.5	0.96	
B240×t1.75-L1420- S100-NH0	149.0	151.9	0.98	
B240-t1.75-L420-S100-UH	167.8	165.2	1.02	Perforated web – Edge unstiffened section
B240-t1.75-L920-S100-UH	152.7	151.8	1.01	
B240-t1.75-L1420-S100-UH	129.5	131.3	0.99	
B240-t1.75-L420-S100-EH	203.6	201.8	1.01	Perforated web - Edge stiffened section
B240-t1.75-L920-S100-EH	186.3	184.4	1.01	
B240-t1.75-L1420-S100-EH	159.2	156.2	1.02	
		Mean	0.996	
		Standard Deviation	0.020	

Accepted / Not Edited

Table III. Material properties for parametric specimens

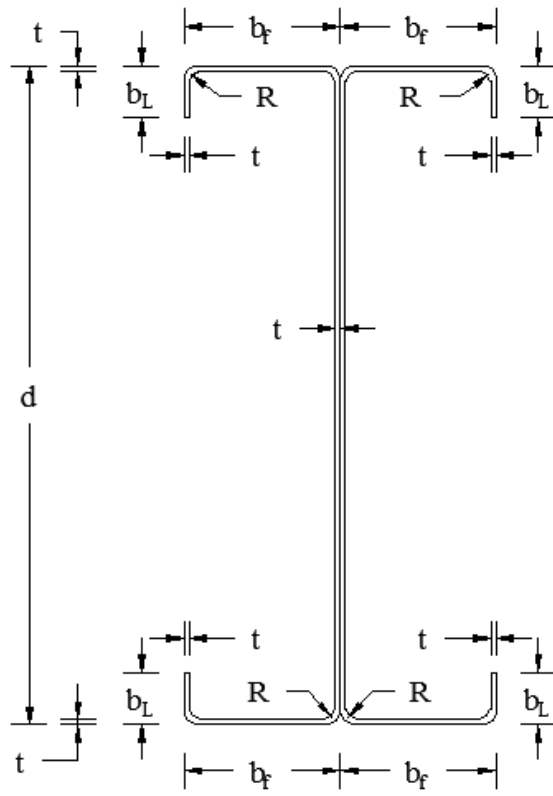
Section	E N/mm²	$\sigma_{0.2}$ N/mm²	σ_u N/mm²
C190×45×15	200000	285.97	385.44

Accepted / Not Edited

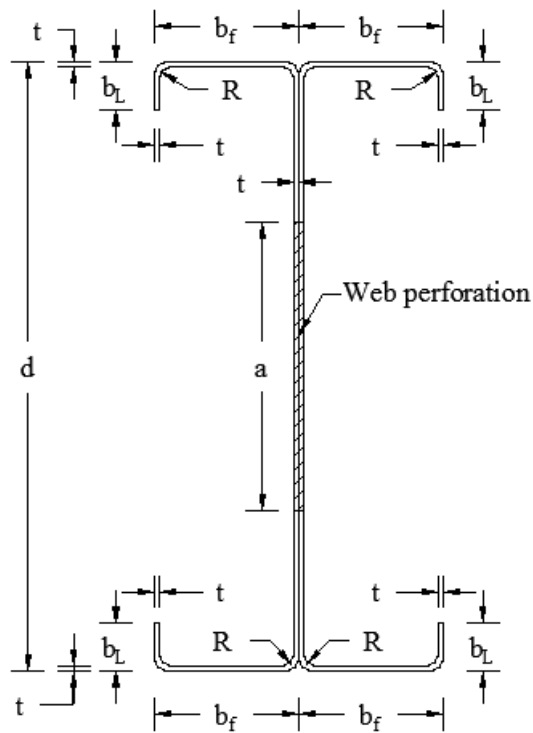
Table IV. Ultimate load of parametric specimens

Specimen ID	P_{U-FEA} (kN)	P_{U-BS} (kN)	P_{U-FEA} / P_{U-BS}	Remarks
B190×45×15-t1.6-L750-NH0	160.28	143.49	1.117	Plain section
B190×45×15-t1.6-L1300-NH0	135.20	130.44	1.036	
B190×45×15-t1.6-L1500-NH0	118.92	124.85	0.953	
B190×45×15-t1.6-L750-UH1	137.50	139.59	0.985	Perforated web – Edge unstiffened section
B190×45×15-t1.6-L1300-UH1	124.95	124.96	1.000	
B190×45×15-t1.6-L1500-UH1	96.60	118.53	0.815	
B190×45×15-t1.6-L1500-UH3	94.91	118.53	0.801	
B190×45×15-t1.6-L1500-UH5	90.34	118.53	0.762	
B190×45×15-t1.6-L1500-UH7	89.80	118.53	0.758	
B190×45×15-t1.6-L750-EH1	163.35	161.50	1.011	
B190×45×15-t1.6-L1300-EH1	148.64	143.52	1.036	
B190×45×15-t1.6-L1500-EH1	157.61	135.55	1.163	
B190×45×15-t1.6-L1500-EH3	166.15	135.55	1.226	
B190×45×15-t1.6-L1500-EH5	167.27	135.55	1.234	
BC190×45×15-t1.6-L1500-EH7	173.45	135.55	1.280	
		Mean	1.012	
		Standard Deviation	0.1725	

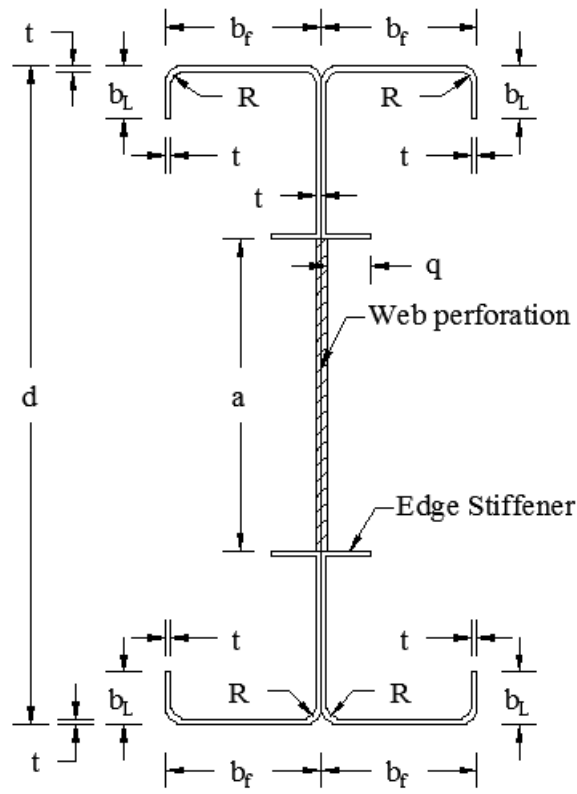
**NUMERICAL INVESTIGATION ON BEHAVIOUR OF COLD-FORMED STEEL
BUILT-UP COLUMN WITH WEB PERFORATIONS**



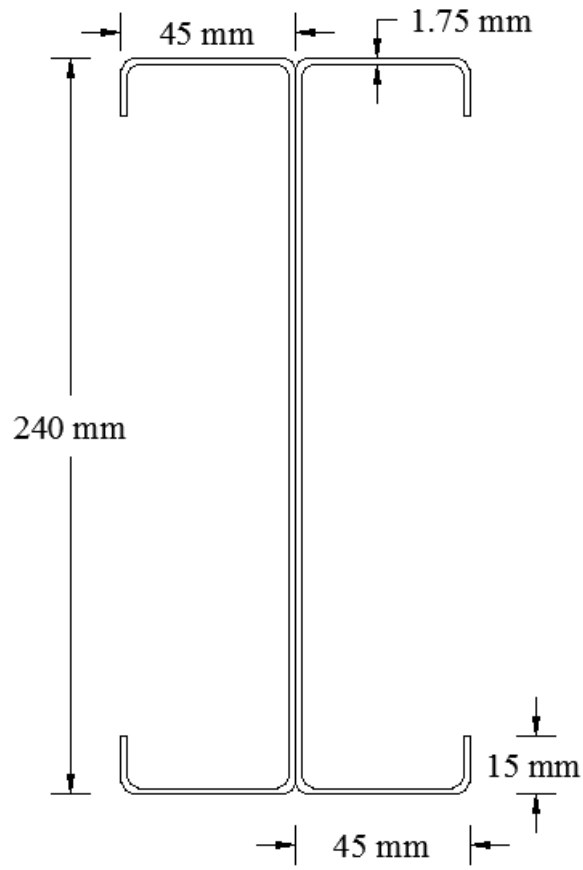
(a). Back-to-back channels



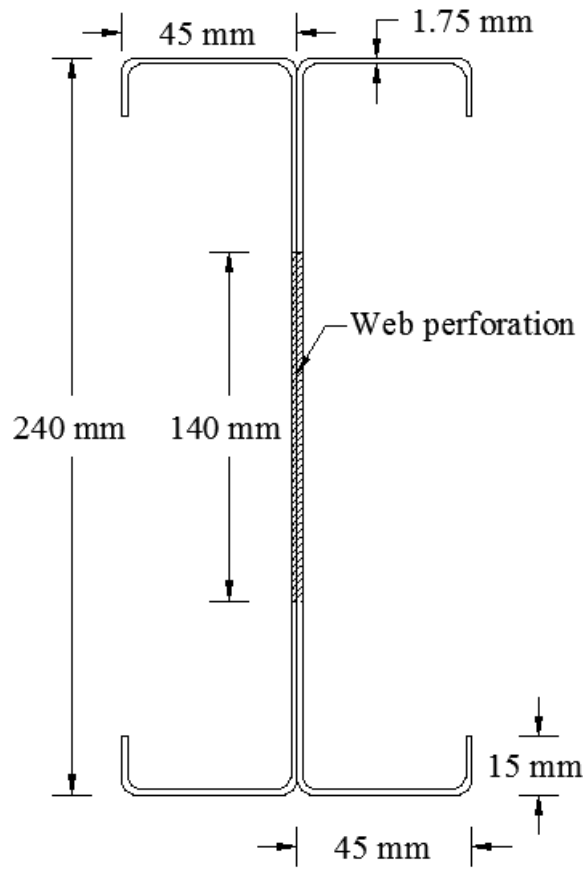
(b). Built-up channel with un-stiffened holes



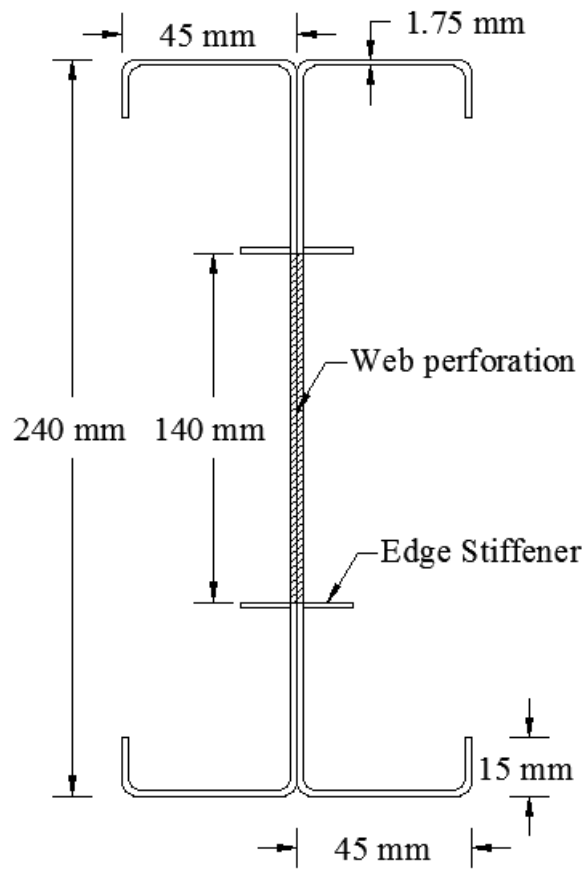
(c). Built-up channel with edge-stiffened holes
 Figure 1. Cross section of built-up channel sections



(a) B240×t1.75-L420-S100-NH0

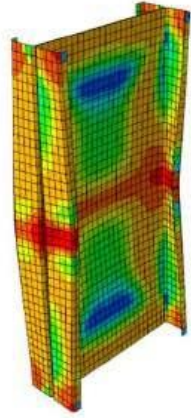


(b) B240×t1.75-L920-S100-NH0

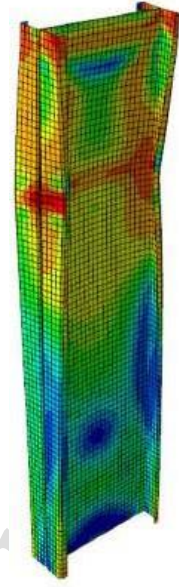
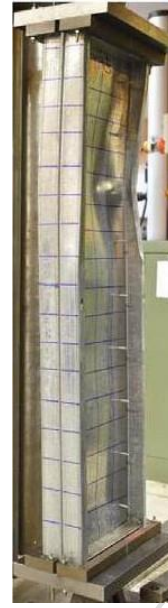


(c) B240x1.75-L1420-S100-NH0

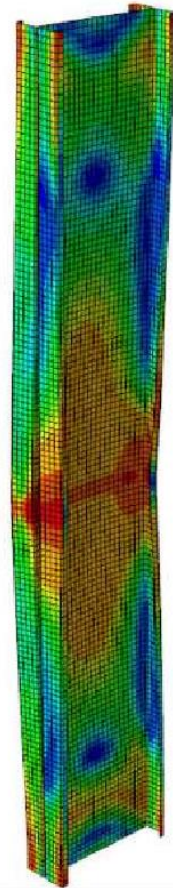
Figure 2. Cross sectional dimensions of validated sections - Chen et al. (2020a)



(a) B240×t1.75-L420-S100-NH0

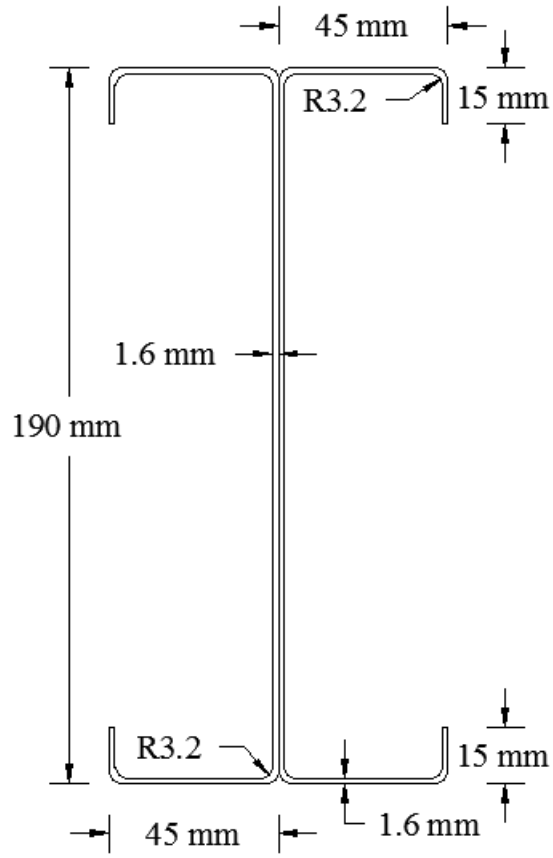


(b) B240×t1.75-L920-S100-NH0

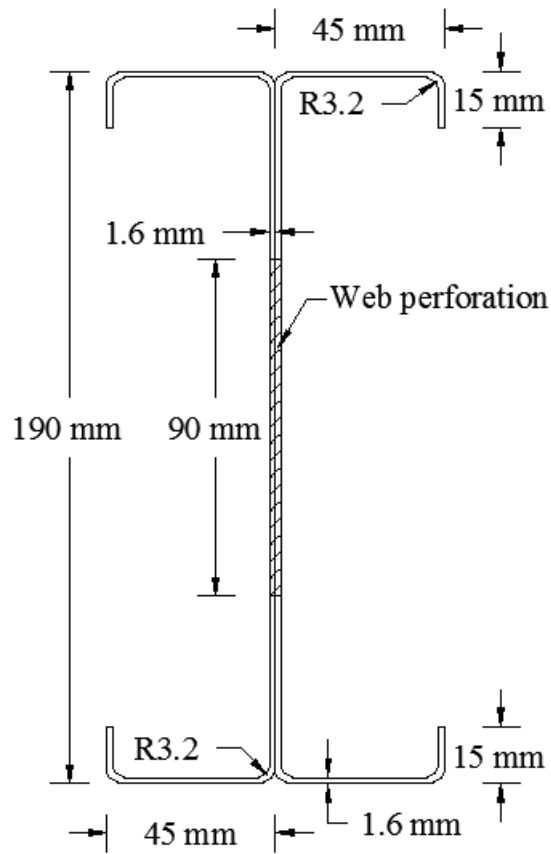


(c) B240×t1.75-L1420-S100-NH0

Figure 3. Buckled shape of validated specimens with FEA - Chen et al. (2020a)



(a) Back-to-back channels



(b) Built-up channel with un-stiffened holes

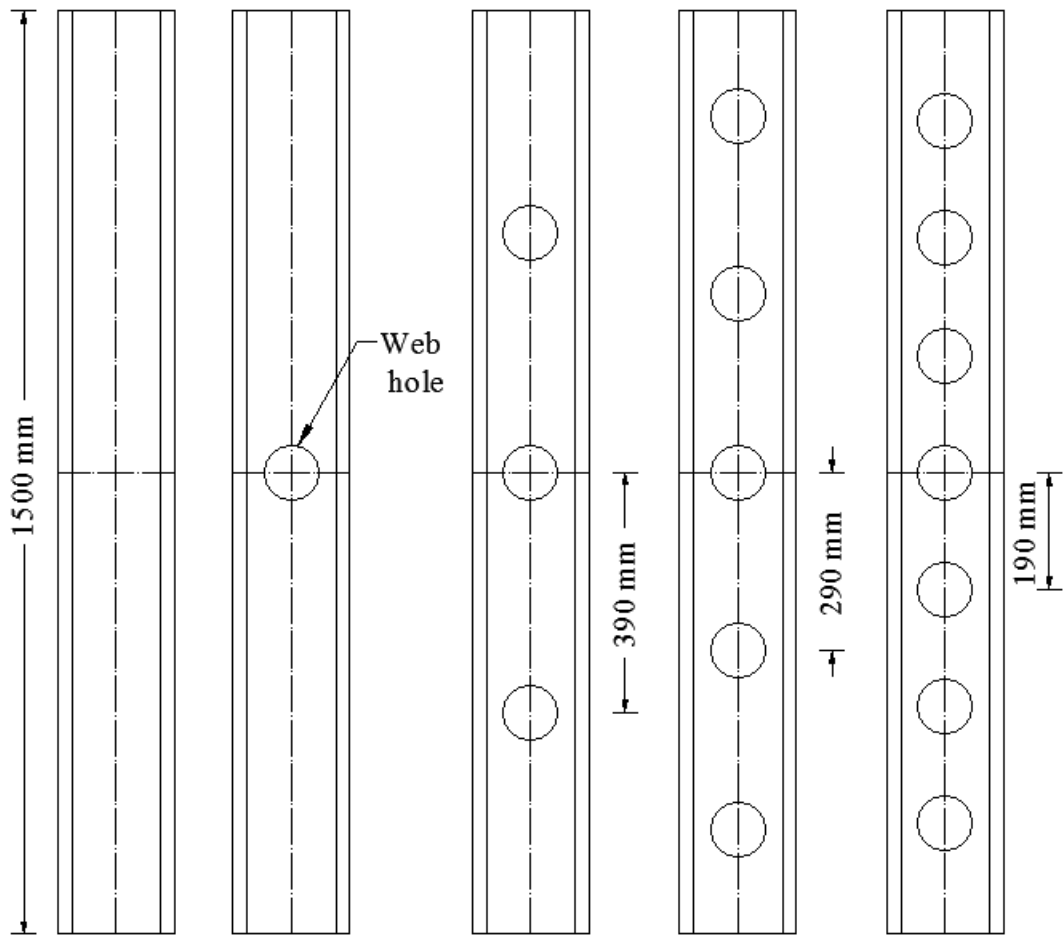


Figure 5. Perforated locations for the parametric sections

Accepted

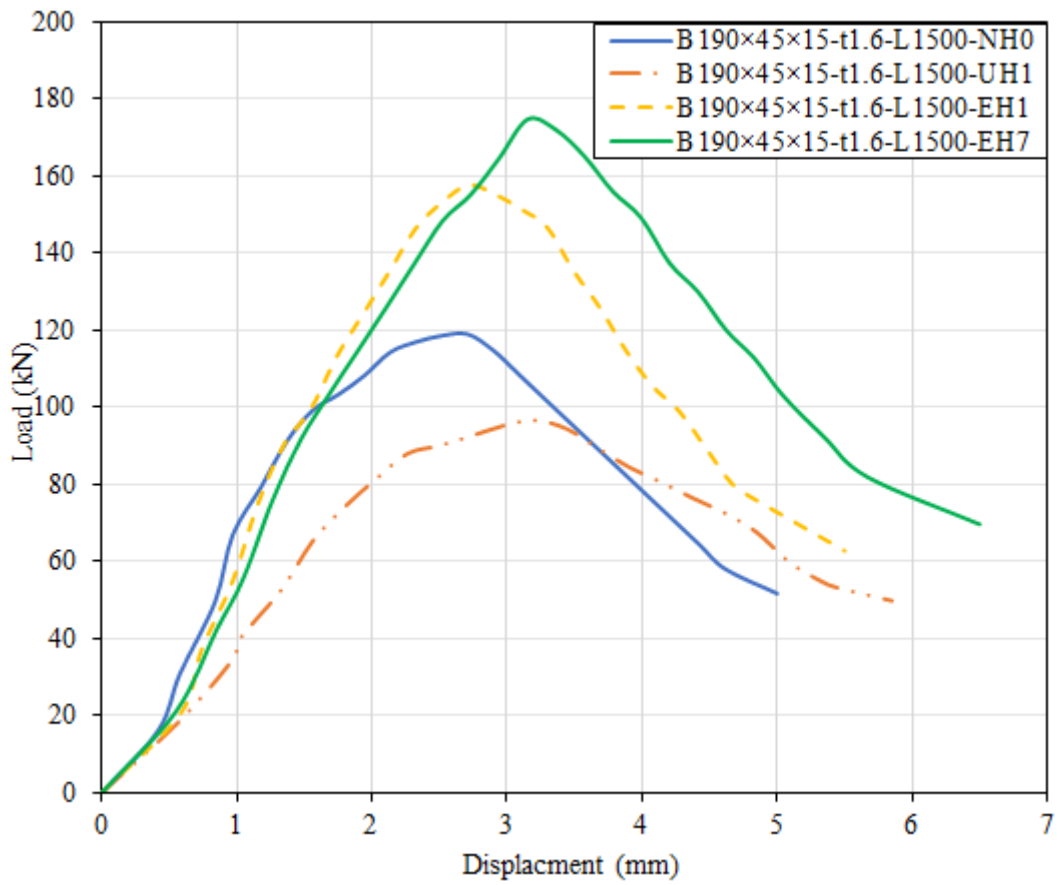


Figure 6. Axial shortening vs axial load (critical section comparison)

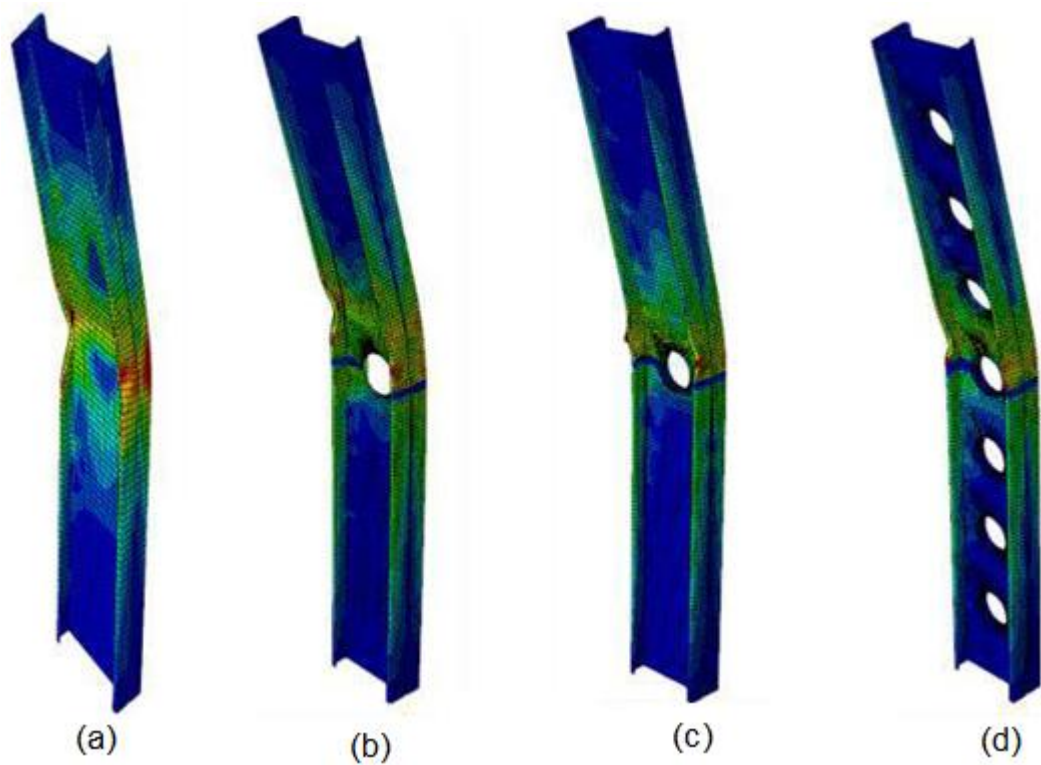


Figure 7. Buckling mode of parametric sections
(a) B190×45×15-t1.6-L1500-NH0,
(b) B190×45×15-t1.6-L1500-UH1,
(c) B190×45×15-t1.6-L1500-EH1,
(d) B190×45×15-t1.6-L1500-EH7.

Accepted